SUBMOLECULAR IMAGING OF EPITAXIALLY CRYSTALLIZED HELICAL POLYOLEFINS BY ATOMIC FORCE MICROSCOPY

W. STOCKER[1], J. C. WITTMANN, A. J. LOVINGER[2], B. LOTZ

Institut Charles Sadron (CRM-EAHP), CNRS and Université Louis Pasteur
6, rue Boussingault, F-67083 Strasbourg, France

[1]Present address: Institut für Physik, Humboldt-Universität zu Berlin
Invalidenstr. 110, D-10115 Berlin. Germany

[2]AT&T Bell Laboratories, 600 Mountain Avenue, Murray Hill
New Jeresey 07974

ABSTRACT. Iso- and syndiotactic polypropylene, epitaxially crystallized on organic substrates are investigated by atomic force microscopy AFM, electron microscopy EM and electron diffraction ED. AFM pictures with high resolution could be obtained when using an environmental liquid cell and probing the sample immersed in water. AFM reveals *both* the lamellar structure *and* large arrays of submolecular methyl groups in unfiltered images. These groups have been visualized by AFM, thus providing the first direct observation of individual *left* and *right* handed polyolefine helices embedded in their crystallographic environment. Epitaxial crystallization appears as a well adapted preparation technique for AFM examination of polymers.

1. INTRODUCTION

Atomic force microscopy AFM (1-2) has proven a very powerful tool to determine the structure and molecular packing of crystalline polymers (3-8).We summarize here some of our work on isotactic and syndiotactic polypropylene (iPP, sPP) oriented by epitaxial crystallization on suitable organic substrates. Epitaxial crystallization involves contact planes in which the polymer chains lie with their helix axes parallel to the substrate surface (9-10). After dissolution of the substrate, the exposed contact surface of the epitaxially crystallized film is highly suitable for AFM examination.

The structure of epitaxially crystallized iso- and syndiotactic polypropylene has been determined by electron microscopy EM and electron diffraction ED: chain conformation, crystal structure and chirality of constituting helices (10, 16-18). In the present investigations, high resolution AFM imaging is used to reveal further structural aspects that are beyond reach of electron microscopy and diffraction techniques.

Atomic resolution AFM images can be obtained when probing the sample in a liquid environment. As shown by Ohnesorge et al. (11), true atomic resolution on inorganic crystals can only be achieved when the estimated net repulsive loading force exerted by the sample on the front atoms of the tip is 10^{-10} N or lower. In the results presented in (11), well defined defects were observed with atomic scale lateral resolution.

The object of this paper is to give an account of the present capabilities of AFM to determine the molecular and submolecular structure of epitaxially grown polymer films: when probing the films immersed in water, lamellar *and* molecular resolution can, in certain cases, be reached together (6, 8). Epitaxial crystallization on organic substrates appears as well adapted sample preparation technique for AFM investigations of crystalline polymers.

2. EXPERIMENTAL

2.1. ATOMIC FORCE MICROSCOPY

AFM experiments were carried out with a Nanoscope III instrument from Digital Instruments, Inc., Santa Barbara, Cal. USA. Images were taken with an A-type scan head (max. scan size 700 x 700 nm^2) equipped with Si_3N_4 tips attached to a microfabricated cantilever (triangular base, 200 μm) with a force constant of 0.06 N/m. With the help of an optical microscope (Nikon OM 240-M11) with xy-adjustable AFM stage, the tip was positioned close to the surface of preselected oriented regions. The zones of interest, usually in the range of 10 x 10 μm^2, are easily located under the optical microscope.

The liquid cell was used as indicated by the supplier. Various liquid media have been tested: benzylalcohol, methanol and water, which are all non solvents of the polymer at room temperature. Water was found most convenient to use and was adoped as a standard environmental medium. For each of the presented AFM images, a set of experiments under different scan parameters was done. The calibration of distances was underevaluated by about 10%. Probing polymers in liquid eliminates the capillary forces caused by water films on the surface. The AFM force curves show less hysteresis in water than in air. Therefore, images could be recorded at any desired separation *d* between the tip and the sample. The higher resolutions were only achieved when minimizing the loading force much smaller than 10^{-10} N, as determined from the force curves.

High resolution images were recorded in the deflection imaging mode. During imaging, no bandpass filters were applied. In order to obtain submolecular resolution, the tip was slowly moved towards the sample until some contrast would be observed. Maximum height modulations of 2 - 3 Å were detected in the atomically resolved images. Scanning line frequencies were 1 Hz for large scale scans (when imaging the lamellar structure) and up to 57 Hz for atomic resolution. Oriented regions with general orientation of lamellae were localized first at a scan size of 500 x 500 nm^2. When zooming inside these areas, reproducible pictures were obtained which show both the lamellar and the molecular structure.

2.2. ELECTRON MICROSCOPY AND DIFFRACTION

Electron microscopy and electron diffraction are performed with a Philips CM12 electron microscope equipped with a geometric stage on essentially the same films as used for AFM investigations. Whereas in AFM the films are used without further processing, they are shadowed for EM observations with Pt/C at an angle of $\tan^{-1} = 1/3$ and coated with a carbon supporting layers.

2. 3. MATERIALS AND SAMPLE PREPARATION

2.3.1. Isotactic polypropylene. The substrate materials, mainly benzoic acid, anthracene or nicotinic acid are of commercial origin. The iPP sample used was provided by SNEA(P). It has 96 % isotactic triads and its molecular weight is 3.8 x 10^3 with polydispersity = 5.2. Epitaxy of iPP on benzoic acid or anthracene substrates produces thin films used for AFM investigations. The films are obtained by comelting the polymer and the substrate between cover glasses and crystallized by sliding on a Kofler hot bench. After separation of the cover slides, the substrate is dissolved in methanol.

*2.3.2. Syndiotactic polypropylene.*Two different syndiotactic polypropylenes were provided by T. Simonazzi of Himont, Ferrara, Italy and P. Agarwal, Exxon Chemical International, Inc., Belgium. The crystallization procedure involved several steps (8). The organic substrate materials are p-terphenyl (3ϕ) and p, p-quaterphenyl (4ϕ) of commercial origin. A thin film of sPP was deposited onto a glass cover slide by evaporation at ~140°C of a dilute solution (0.1% w/v) of the polymer in p-xylene. Single crystals of 4ϕ were prepared from p-xylene and deposited on top of the polymer film.

This composite material was heated to ~160°C and recrystallized by cooling at a controlled rate (−20°C/minute). The oligophenyl substrate crystals were dissolved away with hot amylacetate. The contact surfaces, which can be easily located by the imprint left by the substrate crystals in the polymer film are highly suitable for AFM investigation.

3. CHAIN CONFORMATION AND CRYSTAL STRUCTURE OF TACTIC POLYPROPYLENES

3.1. ISOTACTIC POLYPROPYLENE

3.1.1. *The α-phase of iPP.* The α-phase crystal structure of iPP is well established (12-14). It is based on ternary helices with 6.5 Å chain axis repeat distances. These helices are packed in a monoclinic unit cell with parameters a = 6.65 Å, b = 20.78 Å, c = 6.5 Å and β = 99.6°. The packing is characterized by the alternation of (010) layers made of antichiral helices (Fig. 1).

In c-axis projection (center bottom of fig. 1), the triangles that present the 3_1 helices have one of their bases parallel to the (010) plane, with bases of successive (010) layers facing each other. Therefore, every (040) growth plane differs from its neighbours since alternately two methyl groups or only one point to the outside of the observed surface.

Successive lateral faces A and B thus differ widely in terms of methyl group density and arrangement (left and right of Fig. 1). For each contact plane A and B, two possible arrangements of methyl groups exist depending on the hand of helices in the observed crystallographic plane. This results in two possible patterns in the (040) planes which differ in their symmetry, a feature that is easily accessible to Fourier analysis.

Electron diffraction experiments cannot indicate, which one of the two possible (040) faces interacts with the substrate crystal. We will show that AFM, when it reaches methyl group resolution, can settle this issue.

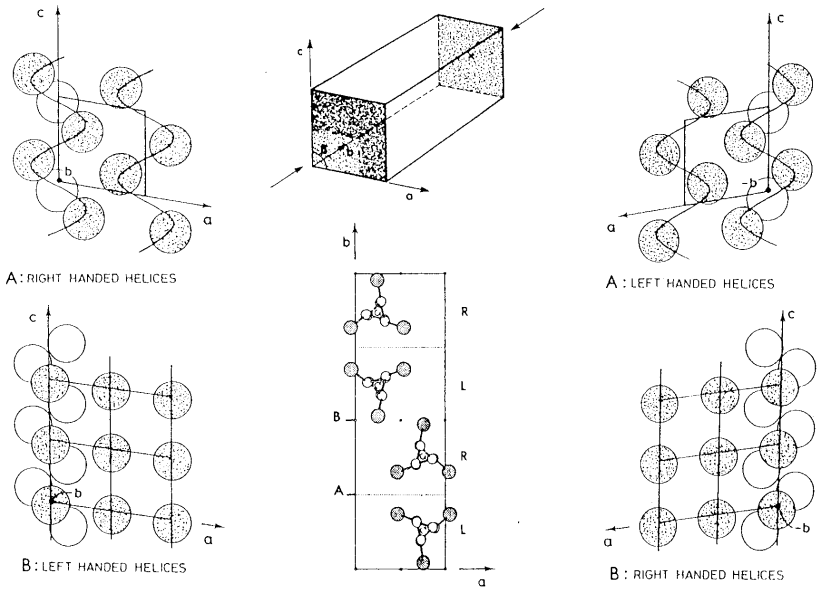

Figure 1. Crystal structure of α-iPP and different (040) contact planes. Center bottom: crystal structure seen in c-axis projection. The triangles represent the 3_1 helices. Note the alternation of left (L) and right (R) handed helices along the b-axis. Since the two helix types have different azimutal settings, two types of (040) lateral faces exist, which are marked A and B. Possible contact faces A and B as seen along the +b and -b directions (cf. center top) are shown in the left and right of the figure.

3.2 SYNDIOTACTIC POLYPROPYLENE

Crystal structure of sPP. The unit cell of syndiotactic polypropylene, first proposed by Corradini et al. (15) is orthorhombic, with helices of the same hand (either all left or all right). It is a C-centered cell with a *b* parameter of 5.7 Å (Fig. 2a). Recent work (16) showed that the stable structure of sPP has unit cell III (Fig. 2b), with the *b* parameter doubled to 11.2 Å. The new cell is based on a strict alternation of left and right handed helices along both *a* and *b* axes and results in a highly symmetrical space group (Ibca). In actual crystals both packing schemes coexist leading to intermolecular lattice disorder. This structural disorder becomes more and more prominent as the crystallization temperature decreases, as shown by Lovinger et al. (18).

Computer generated models of sPP helices in their t_2g_2 conformation (t = trans, g = gauche) are shown in Fig. 3. Note that the prominent rows of CH_3 CH_2 CH_3 groups, which mimic an "n-pentane segment" in its all trans conformation, are tilted at 45° to the helical axes, thus revealing unambiguously the helical hand.

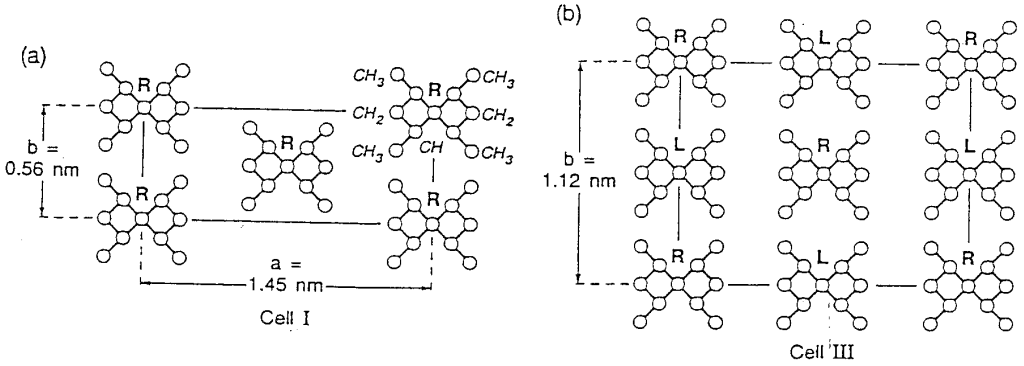

Figure 2. Crystal structure of syndiotactic polypropylene: Two unit cells proposed for the stable form of sPP, as shown in the c-axes direction. (a) C-centerd Cell I with isochiral chains (Corradini et al (15)). (b) body centered cell III with altenation of right (R) and left (L) helical hands along both a and b axes.

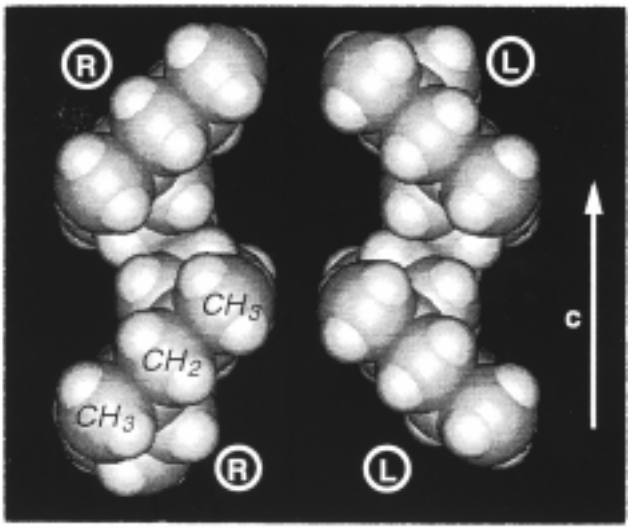

Figure 3. Computer-generated molecular models of right and left handed sPP helices in $(t_2g_2)_2$ conformation as seen along the crystallographic a-axis. Note the prominent rows of CH_3 CH_2 CH_3 groups at 45° to the helical axis (from ref. 8).

4. RESULTS

4.1. SPHERULITE STRUCTURE

Spherulites of sPP. We first examine the overall morphology of sPP obtained on cooling a molten thin film produced by evaporation of a p-xylene solution (0.1 % w/v). sPP produces spherulites with radial lamellae.

Fig. 4 (a-b) show a typical spherulite structure which is well known from electron microscopy and optical microscopy. Crystalline polymers cannot be obtained in the form of macroscopic single crystals as they form thin, chain folded lamellar crystals or (in bulk) spherulites made up of radiating lamellae with tangential orientation of the chains.

In the spherulites observed in Fig. 4, each of these radially arranged fibrils consists of small lamellar crystals. Several chain orientations thus exist in these films. High resolution AFM imaging on such polycrystalline material is difficult since the crystallites with single orientation of chains are very small. For AFM examination therefore, preparation techniques which induce a more regular orientation of the polymer molecules have to be applied. One such method rests on epitaxial crystallization of the polymers.

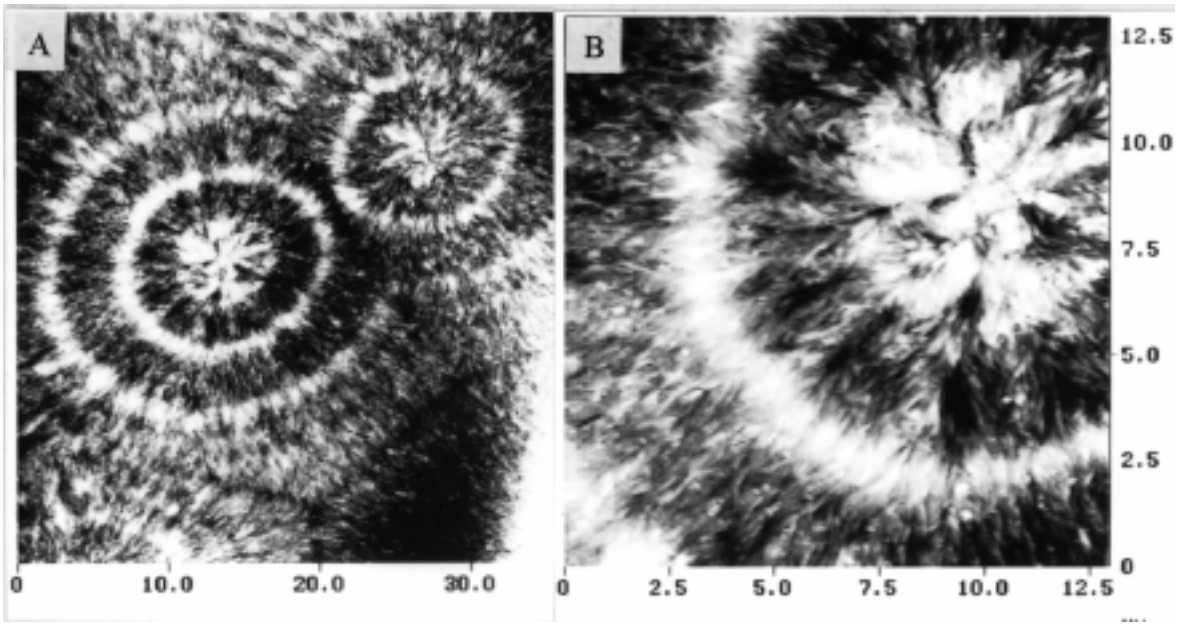

Figure 4. AFM images of sPP spherulites obtained on a thin film produced by evaporation of a p-xylene solution (a) 40 μm x 40 μm, (b) 12 μm x 12 μm; grey scale 180 nm (a-b)

4.2. EPITAXY AND CHAIN ORIENTATION

4.2.1. Contact faces and lamellar orientation. Epitaxial crystallization of iPP and sPP on suitable organic substrates makes it possible, after dissolution of the substrate, to expose the contact plane in which the polymer chains lie with their chain axes parallel to the surface. The substrates used are benzoic acic, nicotinic acid or anthracene for iPP and p-terphenyl or p-quaterphenyl for sPP.

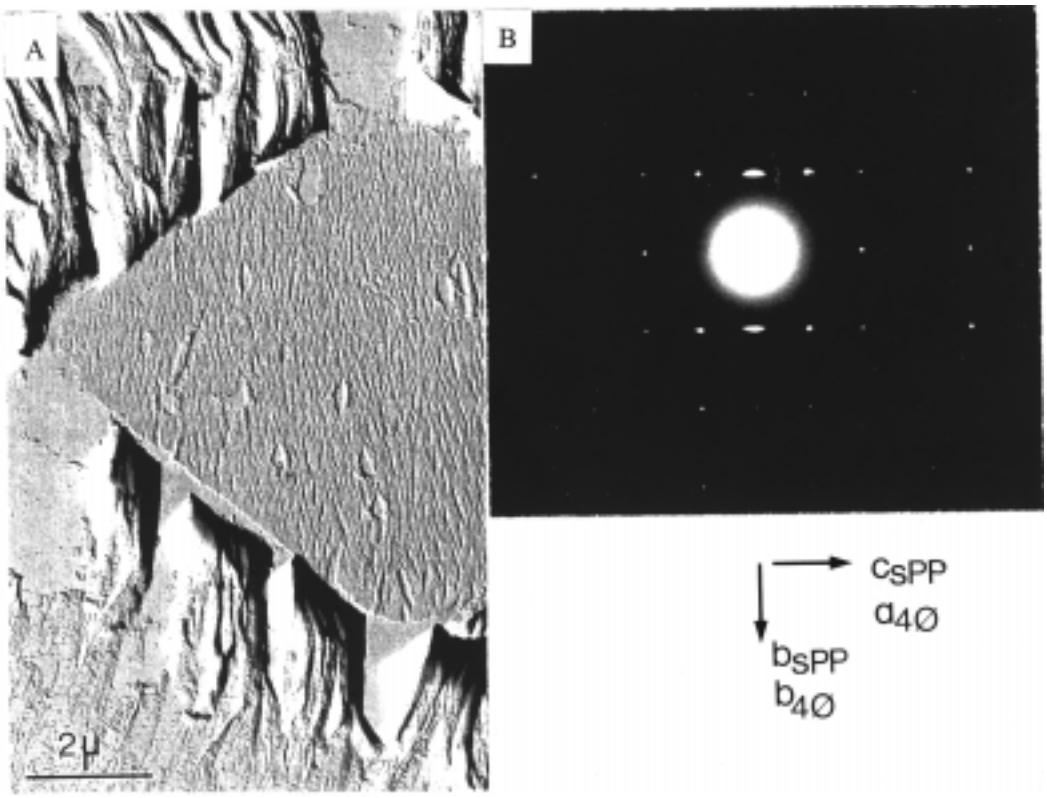

Figure 5. Contact-faces of sPP films obtained by epitaxial crystallization on the (001) face of a p, p-quaterphenyl substrate crystal after dissolution of the substrate. (a) Transmission electron micrograph, Pt-C shadowed at $\tan^{-1}$ = 1/3, scale bar = 2 μm. Note the general orientation of lamellae along the short diagonal of the substrate crystal and the imprint left by the latter, which helps to locate oriented areas. (b) Composite electron diffraction pattern of a p, p-quaterphenyl (4ϕ) substrate crystal (sharp diffraction spots) and the sPP film epitaxially crystallized on this substrate (arced reflections) with respective orientations indicated. The polymer chains are oriented parallel to the a-axis of the substrate (from ref. 8).

As an illustrative example, Fig. 5a shows the transmission electron microscopic picture of a sPP film, epitaxially crystallized on p-terphenyl. The oligophenyl substrate crystal was subsequently dissolved away with hot amyl acetate. Note the *general orientation of lamellae* along the short diagonal of the substrate crystal and the imprint in the polymer left by the substrate. These "contact surfaces" of epitaxially crystallized films are highly suitable for AFM examination. The original substrate position is still detectable by the imprint of its external contour in the sPP film. The polymer contact face is exposed. Fig. 6 shows the corresponding large scale AFM image, taken in the oriented region of Fig 5a. The brighter rows are separated equidistantly by a periodicity of 14 nm, which is the average lamellar thickness of sPP determined from EM and small angle ED. Note the existence of lamellar defects. The dark regions in fig 6 correspond to the interlamellar regions which are visible in epitaxially crystallized films since lamellae stand edge on.

4.2.2. Epitaxy and lattice matching. The polymer-substrate epitaxial relationship can easily be established by wide angle electron diffraction where the sharp spots correspond to the substrate crystal 4ϕ and the broader arcs to the polymer crystal sPP (fig. 5b). Note the single orientation of polymer chains. Quantitative analysis of this diffraction pattern is equally straightforward: The polymer chains lie with their chain axes *parallel to the a axis of* the substrate. The lattice matching is two dimensional. Using room temperature crystallographic parameters it amounts to –8.1 % in the chain direction and 0.9 % perpendicular to the chains.

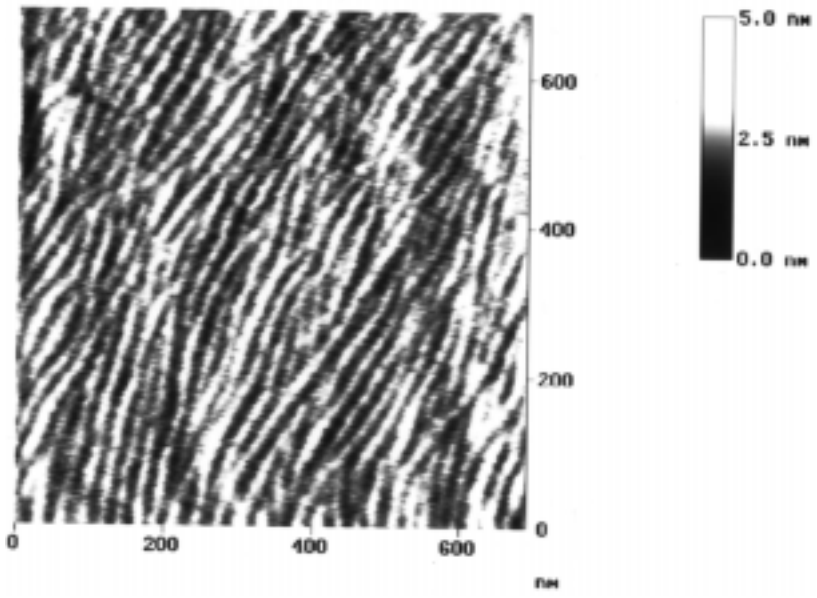

Figure 6. Lamellar morphology (edge on lamellae) obtained in the oriented region 5 (a) revealed by AFM. The brighter rows are seperated equidistantly by 14 nm spacing.

4.3. MOLECULAR PACKING AND DIRECT OBSERVATION OF THE HELICAL HAND

4.3.1. Isotactic polypropylene. High resolution AFM images (taken in a liquid environment) of the contact surface of iPP, epitaxially crystallized on anthracene are shown in Fig 7 (a-b). The resolution was only achieved by minimizing forces between tip atoms and polymer surface to values smaller than 10^{-10} N. At higher forces (decreasing tip sample separation), the atomic corrugation gradually disappears.

Fig. 7 a shows one of a set of experiments which are reproducible revealed at various scan parameters (scan rate, scan size scan angle). The lamellar and chain orientations (determined by EM and ED) are indicated by arrows. A nearly square pattern of methyl groups is apparent in the unfiltered AFM image (Fig 7a). Furthermore, the picture shows darker bands (vertical in Fig. 7a). From their spacing and general orientation relative to the methyl group pattern they correspond to the interlamellar regions.

The two dimensional Fourier transform (2D-FFT) of Fig. 7a reveals both, *small angle* and *wide angle* patterns (Fig. 7b). The six spots wide angle pattern are expected from the nearly square pattern of methyl groups with one pair of (001) and one pair of (100) spots (both at 6.5 Å spacing) and one pair of (101) spots. The small angle part of the pattern corresponds to the 120 Å spacing of the dark bands (Fig. 7a) and supports its assignment to the lamellar periodicity.

The observed lamellar and methyl group organization (Fig. 7 a-b) indicate that the contact plane with lower density of methyl groups (face B) interacts with the substrate. The result is unambiguous since the patterns of A and B faces differ in their symmetry, a feature that is easily accessible to Fourier analysis. Furthermore, the arrangement of methyl groups relative to the lamellar surface clearly corresponds to the situation depicted at the bottom left of Fig. 1 and the imaged helices in the exposed (040) plane are all left handed. The six "wide angle" spots in the 2D-FFT (Fig 7b) and their organization relative to the lamellar orientation indicate the hand of helices which bear the observed methyl groups.

As described in (5, 7), epitaxy of iPP on organic substrates investigated so far always leads to face B in the observed contact surface. Furthermore, the α-phase and a different γ-phase of iPP are distinguishable by their helix axes orientation with respect to the lamellar surface.

4.3.2 Syndiotactic polypropylene. High resolution AFM pictures of sPP films have been obtained in the oriented region shown in figures 5a and 6. Fig. 8a illustrates one out of several sets of comparable images obtained in this study. The helix axes orientation -known from the lamellar organization in the corresponding large scale AFM pictures- is indicated by an arrow in Fig 8a. The arrangement of individual "n-pentane segments" tilted at 45° to the helical axes is clearly visible in the unfiltered AFM images in form of elongated features. However, the individual CH_3´s and CH_2´s of these pentane segments are not clearly resolved. The corresponding two dimensional Fourier transform of the unfiltered picture (Fig. 8b) shows more than 20 pairs of spots; the outermost spots correspond to spacings of 1.7 Å, which indicates that methyl group resolution has been reached. Fourier filtered pictures (Fig 8c) display two alternating orientations of CH_3 CH_2 CH_3 stretches tilted at 45° to the helical axes and thus reveal unambiguously the helical hand of constituting helices in the bc contact plane. The CH_3 CH_2 CH_3 substructure of the elongated features is discernible. The picture shows a nearly rectangular pattern with dimensions of 1.0 nm perpendicular to the chains and 0.7 nm along the helical axes, consistent with the sPP crystal structure (18).

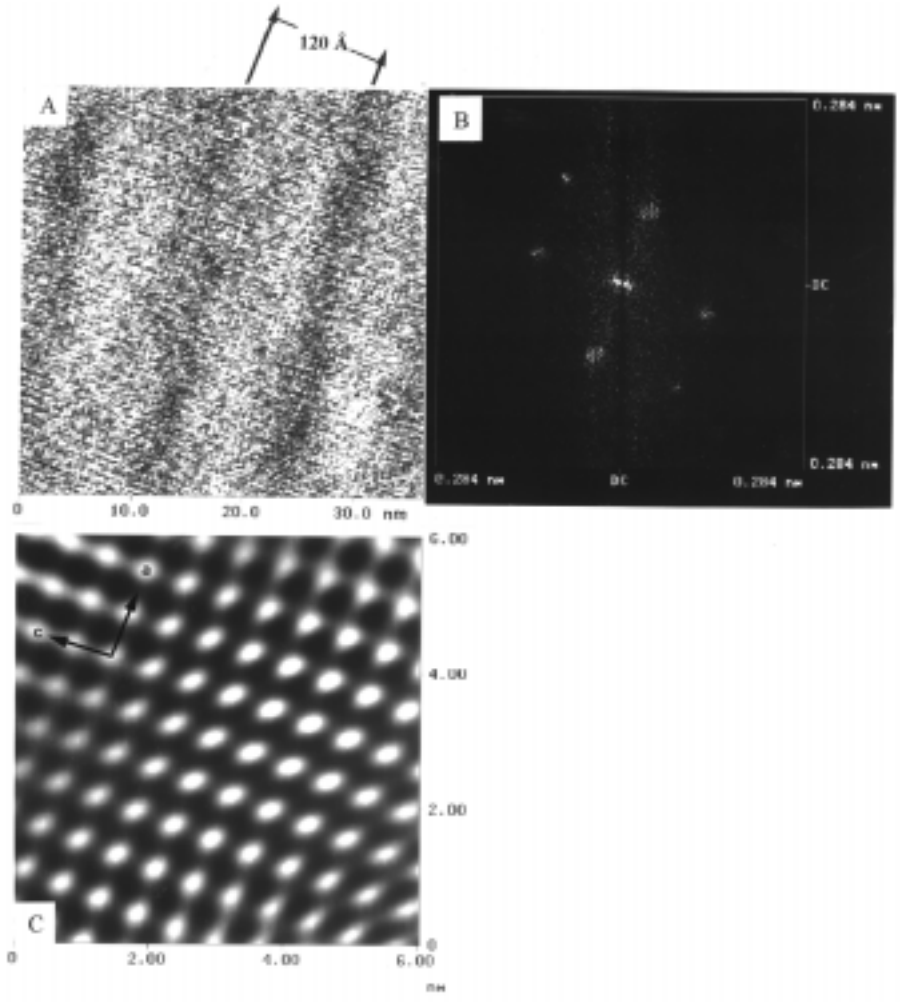

Figure 7. (a) Unfiltered AFM images of the contact surface of an isotactic polypropylene film epitaxially crystallized on anthracene. The nearly square pattern of methyl groups (6.5 Å spacing) correspond to the (010) plane of the α-phase (cf. Fig 1); lamellar periodicity 120 Å, (b) Two dimensional Fourier transform of the unfiltered image in (a). Note the presence of both low angle and wide angle maxima, corresponding to lamellar (120 Å) and unit cell (6.5 Å) surface pattern. (c) Enlarged Fourier-filtered image of Fig 7a using the six wide angle spots in Fig. 7b. The chain orientation c is indicated by an arrow. Note the pattern of methyl groups similar to that of the contact face B in Fig 1 (from ref. 6).

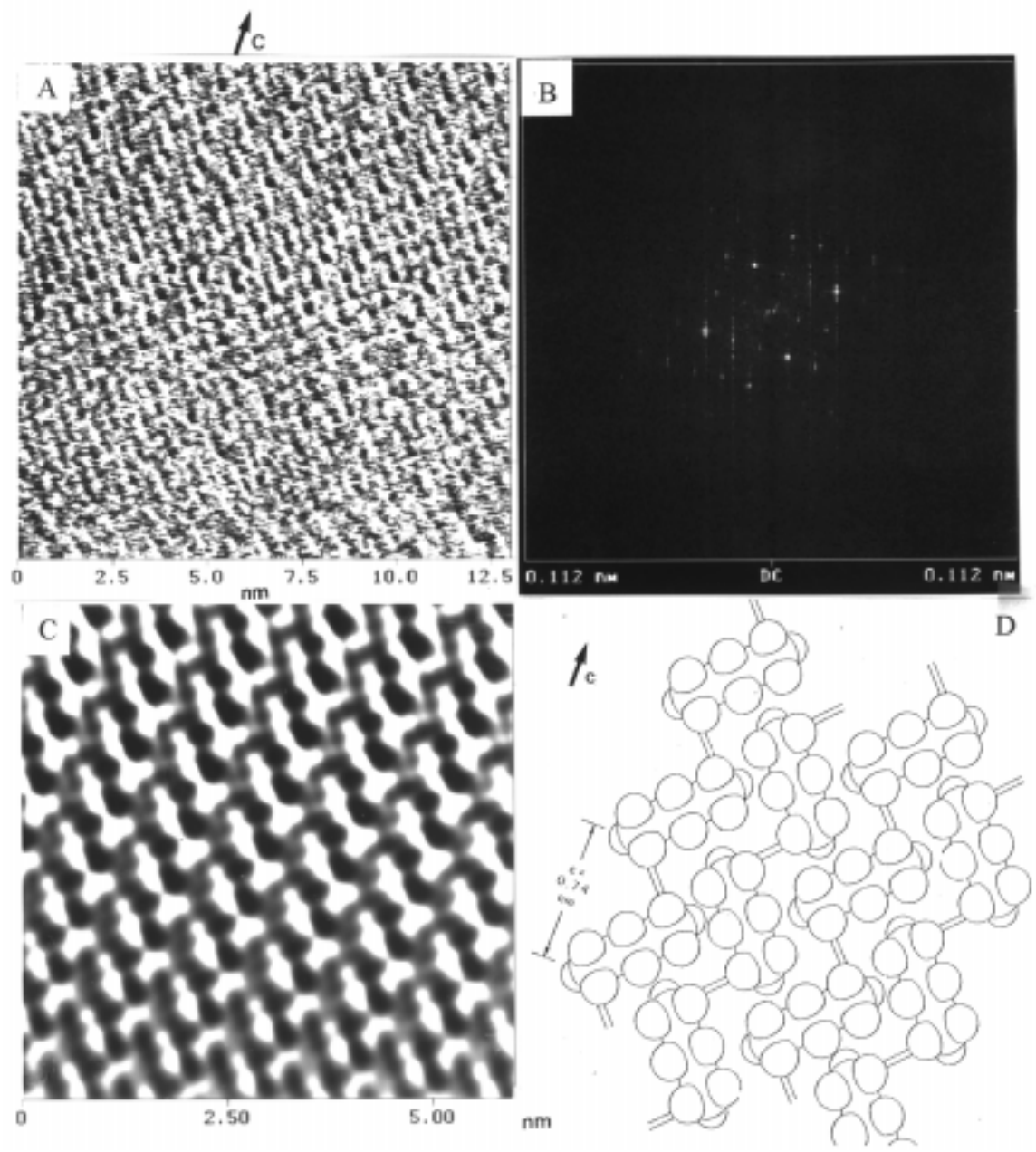

Figure 8. High resolution AFM images of syndiotactic polypropylene, epitaxially crystallized on p,p-quaterphenyl. The chain axes orientation c (known from the lamellar orientation in the large scale AFM image in fig. 5c) is indicated by arrows. Note the existence of elongated features tilted at 45° to the helical axis orientation. (a) unfiltered AFM image. (b) Two dimensional Fourier transform of (a). (c) Fourier filtered image of (a) produced when selecting twenty pairs of spots in the power spectrum in (b). Note the better resolution of CH_3 CH_2 CH_3 tilted at 45° to the helical axes which indicate the helical hand. (d) Schematic representation of the AFM image in (c) using molecular modeling, shown in the correct mutual orientation, Cell III of fig. 2 (b), space group Ibca (from ref. 8).

4.4. DISCUSSION

4. 2. 1. The nature of the contact face. The contact face usually corresponds to the densely packed crystallographic plane which is dictated by structural and lattice matching between polymer and substrate. This plane is determined by electron diffraction experiments. As an illustration, Fig. 5b shows the pattern corresponding to Fig. 5a. It indicates that the sPP contact plane is bc. The present study shows very high resolution (i. e. methyl group) on a relatively large scale. It is therefore possible to visualize *lamellar and chain* features in the same image.

4.4.2. Tip geometry and resolution of chains. One feature of Fig. 7a indicates that we may not have the "ideal" image of the surface. In many cases the pattern of methyl groups appears not only on the lamellar core surface but also, less prominently, in the darker bands which we associate with the interlamellar regions which include amorphous material. In these cases, the methyl group topography is not realistic beyond the lamellar edge and indicates that more than one site of the tip contributes to forming the image. As the tip is scanned over the lamellar edge, the point of closest range with the sample starts to shift until another part of the tip interacts with the sample. Due to this "tip switch", the pattern of methyl groups is artificially smeared into the interlamellar regions. Further lowering of the feedback parameters and finding an optimum scan rate can help to eliminate this instrument-generated artifact.

The quality of tip can easily be checked by turning the sample with respect to the tip. As shown by EM and ED, the observed epitaxially crystallized films show a *single orientation of chains* over a wide area of 10 x 10 μm^2 (cf. Fig. 5-6). This allows us to use the sample as a test material by turning it with respect to the tip and reproduce images. Multipe tip imaging should give different Moiré patterns by rotating the sample (the polymer chains) relative to the Si_3N_4-tip. These Moiré patterns were not observed in the present investigations. Several sets of experiments using different tips were performed under various tip/sample (chain) orientations. Only high quality selected tips give reproducible patterns with similar structures at any chain orientation relative to the Si_3N_4-tip. On this basis, the contact surface of epitaxially crystallized iPP, with its lamellae standing edge on provides a sample that can be used also as quality test material for AFM tips.

5. CONCLUSION

AFM imaging of polymers in a liquid environment yields much improved resolution since reduction of capillary forces makes it possible to use imaging forces in the range of 10^{-10} N or lower. Images can be recorded at any desired separation between the tip and the sample.

The unusually clear AFM images of contact faces of epitaxially crystallized isotactic and syndiotactic polypropylene demonstrate that submolecular resolution of poymer helices is achievable although it is not nearing routine work.

AFM displays structural information on semicrystalline polymers beyond reach of techniques based on diffraction as illustrated in the present case for the structure of contact faces and the helical hand of individual exposed chains. Given its resolution, AFM becomes a powerful tool for problems related to the structure of polymers such as direct determination of helical hand, analysis of packing of chains (chiral or antichiral, parallel or antiparallel, syncline or anticline) or even for imaging packing defects.

Acknowledgement

The authors are grateful to M. Schumacher und S. Graff for their assistance in preparation of sPP-films. W. S. acknowledges support from the Université Louis Pasteur, Strasbourg, and the Centre National de la Recherche Scientifique CNRS.

6. REFERENCES

/1/ G. Binnig, C. F. Quate, C. Gerber, Phys. Rev. Lett. **56**, 930 (1986).

/2/ P. K. Hansma, V. B. Elings, O. Marti, C. E. Braker, Science, **242**, 209 (1988).

/3/ B. Lotz, J. C. Wittmann, W. Stocker, S. N. Magonov, H.-J. Cantow, Polym. Bull. **26**, 209 (1991).

/4/ D. L. Dorset, Chemtracts: Macromol. Chem. **3**, 200 (1992).

/5/ W. Stocker, S. N. Magonov, H.-J. Cantow, J. C. Wittmann, B. Lotz, Macromolecules, **26,** 5915 (1993).

/6/ W. Stocker, S. Graff, J. Lang, J.C. Wittmann, B. Lotz, Macromolecules, **27**, 6677 (1994).

/7/ W. Stocker, S. Magonov, H.-J. Cantow, J. C. Wittmann, B. Lotz, Macromolecules **27**, 6690 (1994) Erratum to ref. 5.

/8/ W. Stocker, M. Schumacher, M. Graff, S. Lang, J. C. Wittmann, A. J. Lovinger, B. Lotz, Macromolecules (1994) in press.

/9/ J. C. Wittmann, B. Lotz, Prog. Polym. Sci. **15**, 909 (1990).

/10/ B. Lotz, J. C. Wittmann, J. Polym. Sci. Polym. Phys. **24**, 1541 (1986).

/11/ F. Ohnesorge, G. Binnig, Science, **260**, 1451 (1993).

/12/ G. Natta, P. Corradini, P. Nuovo. Cimento Suppl. **15**, 40 (1960).

/13/ Z. Mencik, J. Macromol. Sci. **B6**, 101 (1972).

/14/ M. Hikosaka, J. Seto, Polym. J. **5**, 111 (1973)

/15/ P. Corradini, G. Natta, G. Ganis, P. A. Temussi, J. Polym. Sci. Part C, **16**, 2477 (1967).

/16/ B. Lotz, A. J. Lovinger, R. E. Cais, Macromolecules, **21**, 2375 (1988).

/17/ A. J. Lovinger, B. Lotz, D. D. Davis, M. Schumacher, Macromolecules, **27**, 6603 (1994).

/18/ A. J. Lovinger, B. Lotz, D. D. Davis, F. J. Padden, Macromolecules, **26**, 3494 (1993).